ISBN: 978-3-95450-227-1 ISSN: 2673-5490 doi:10.18429/JACoW-IPAC2022-WEPOPT058

A RESPONSE MATRIX APPROACH TO SKEW-SEXTUPOLE CORRECTION IN THE LHC AT INJECTION

E. Waagaard[1], E.H. Maclean, CERN, Geneva, Switzerland
[1]also at Uppsala University, Uppsala, Sweden

Abstract

To date, no dedicated attempt has been made to correct the skew-sextupole (a_3) $3Q_y$ resonance in the LHC at injection. This topic has recently gained interest, following investigation of the emittance growth during the LHC energy ramp due to third-order islands. The LHC is equipped with skew-sextupole correctors in the experimental insertions, intended for local compensation at top energy, and with families of skew-sextupole magnets in the arcs, intended for chromatic-coupling correction (but not optimally placed for $3Q_y$ compensation). Simulation studies were performed to assess whether these correctors could compensate $3Q_y$ in the LHC at injection via a response matrix approach, based on values at the BPMs. Corrections for $3Q_y$ could be found within magnet powering limitations, but required significantly increased corrector strength compared to chromatic-coupling compensation.

a_3 CORRECTION SCHEME

Interest in $3Q_y$ resonance compensation at LHC injection (450 GeV) has arisen, due to potential influence of islands on emittance growth during the ramp [1] and on lifetime or emittance at flat-bottom in conjunction with e-cloud. Unfortunately, while two types of skew-sextupole (a_3) magnet are present in the LHC, the lattice was not designed with $3Q_y$ compensation at injection in mind.

In the arcs, several chromaticity sextupoles (*MS*) are rotated to provide skew-sextupoles (*MSS*) for chromatic-coupling correction. MSS are powered in series arc-by-arc, with 1 family (Arc34) broken and unusable, and are arranged in each arc to suppress their influence on $3Q_y$ [2]. The standard a_3 correction scheme uses MSS to minimize arc-by-arc a_3 errors in LHC main dipoles ('*MB*') weighted by optics functions, based upon magnetic measurements [2, 3]. It takes no account of additional sources (e.g. feed-down). Skew-sextupole strength ($[\mathrm{m}^{-3}]$) is defined for the LHC error model [4]

$$K_{n,skew} = -\frac{1}{B\rho}(n-1)!a_n = -\frac{1}{B\rho}\left.\frac{\partial^{n-1}B_x}{\partial x^{n-1}}\right|_{0,0,s} \quad (1)$$

with $n = 3$. MSS strengths from the standard correction are shown in Fig. 1. Beam-based minimization of chromatic-coupling has also been tested, with comparable order-of-magnitude strengths required [5, 6].

a_3 correctors (MCSSX) are also installed either side of the experimental insertions (IR[1,2,5,8]). MCSSX are intended for local correction of IR errors at top-energy [6, 7], and are not used at injection. Use is complicated by their location in the common insertions, meaning the beams cannot be controlled independently. Crossing and separation bumps also result in feed-down if used in operation.

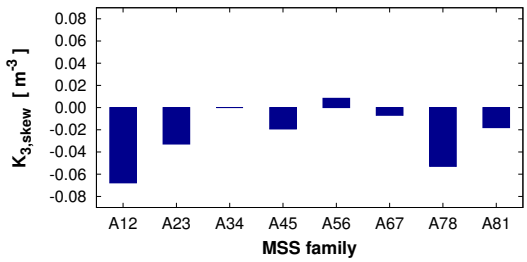

Figure 1: MSS strength for standard a_3 correction scheme.

Maximum MSS and MCSSX powering at 450 GeV are $K_{3,skew} = 6.19\,\mathrm{m}^{-3}$ and $K_{3,skew} = 1.5\,\mathrm{m}^{-3}$.

While neither MSS nor MCSSX were intended for $3Q_y$ compensation at 450 GeV, simulation-based studies were performed to test if they could in principle correct the $3Q_y$ resonance driving term (RDT) f_{0030} using a response matrix approach. Response matrix approaches for sextupole resonances have been employed at PSB [8] and Diamond [9]. Discussion of the simulations and results is given in [10]. An ideal LHC model with no errors was used to construct a response matrix $\mathbf{R}$ of $\mathrm{Re}[f_{0030}(s)]$ and $\mathrm{Im}[f_{0030}(s)]$ to the MSS and MCSSX,

$$\mathbf{R}\vec{\Delta k} = \vec{\Delta f} \quad (2)$$
$$\vec{\Delta f} = (\Delta f_{b1,\mathrm{Re}}, \Delta f_{b1,\mathrm{Im}}, ...\Delta f_{bm,\mathrm{Re}}, \Delta f_{bm,\mathrm{Im}})$$

where only BPM locations ($b1$...bm) are considered, reflecting operational scenarios where correction would be based on measured f_{0030} at BPMs. Models were generated in MAD-X and RDT values calculated via PTC.

Having determined $\mathbf{R}$ from the ideal model, simulations including various linear and nonlinear errors were performed. Modelled RDT values at BPMs ($\vec{f}$) were used to determine corrections via the pseudo-inverse of the response matrix $\mathbf{R}^+$ (calculated by SVD).

$$\vec{\Delta k} = -\mathbf{R}^+\vec{f} \quad (3)$$

$\vec{\Delta k}$ corrections were applied to the previous model, and RDTs re-calculated to test if the correction reduced $|f_{0030}|$. Only the Beam1 response was considered when using the MCSSX. Studies with MCSSX also only considered a flat-orbit (with crossing/separation bumps removed) to limit complications from feed-down.

f_{0030} CORRECTION RESULTS

The response matrix ('$\mathbf{R}$-matrix') approach was effective in simple test cases [10]: correctly identifying mispowered

ISBN: 978-3-95450-227-1 ISSN: 2673-5490 doi:10.18429/JACoW-IPAC2022-WEPOPT058

MSS circuits, and compensating $|f_{0030}|$ generated by single errors. Consequently, models of increasing complexity and operational relevance were considered.

Figure 2 shows $|f_{0030}|$ for a model including only measured a_3 errors in the MB (red). The standard correction of Fig. 1 is also calculated, but deteriorates f_{0030} (green). By contrast $3Q_y$ correction with the MSS significantly reduced f_{0030} (blue). Large jumps at 11 km and 15 km occur in the strong MSS circuits. Correction of $3Q_y$ however, required an order-of-magnitude increase in corrector strength compared to the standard method (MSS were designed to minimally perturb $3Q_y$). Such strong corrections may pose a challenge for operation via deterioration of chromatic-coupling, and further studies of this effect are ongoing.

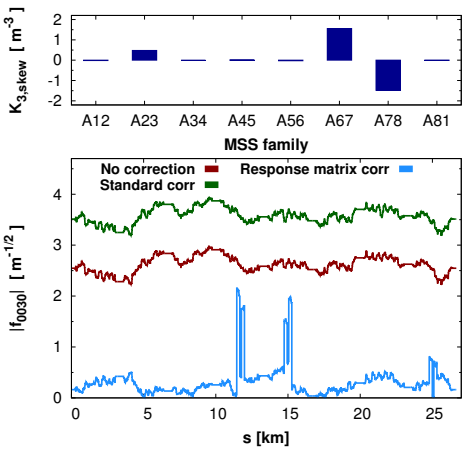

Figure 2: Simulated $|f_{0030}|$ before/after correction (bottom) for model including only a_3 errors in main dipoles, and MSS corrector strengths from response-matrix (top).

Another consideration is whether $3Q_y$ correction is viable with additional error sources. Figure 3 shows $|f_{0030}|$ before/after compensation (dark/light orange) when also including b_2 errors in MB and main quads ('*MQ*'), generating a realistic peak β-beat $\Delta\beta/\beta \approx 10\,\%$. **R**-matrix corrections did reduce the RDT, however $|f_{0030}|$ after correction deteriorated compared to models with only MB a_3 errors. The effect of linear coupling was also non-negligible, and Fig. 3 (dark/light purple) shows $|f_{0030}|$ before/after correction upon inclusion of a_2 errors generating a closest-tune-approach $|C^-| = 0.005$. Introduction of the coupling increased uncompensated $|f_{0030}|$ by $\approx 50\,\%$, with a corresponding deterioration post-correction. While linear optics errors did deteriorate $3Q_y$ correction quality, neither linear-coupling or β-beat represented a fundamental obstacle.

In contrast, Fig. 3 (black) also shows, however, the effect of adding best-knowledge alignment errors of MB, MQ, and MS, into models including all measured non-linear multipole errors (while minimizing orbit, β-beat, and coupling). A large increase to $|f_{0030}|$ is observed. No post-correction result is shown, as required MSS strengths exceeded powering limits. f_{0030} predictions of the model are as yet untested with beam, and studies in Run 3 will aim to benchmark the

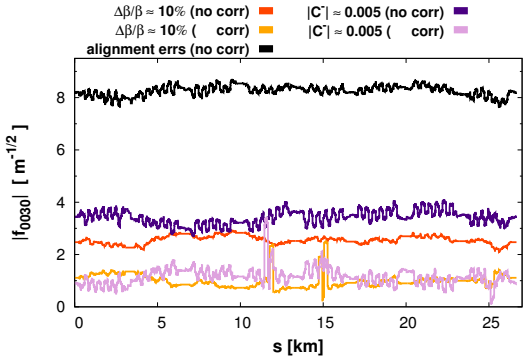

Figure 3: $|f_{0030}|$ before/after **R**-matrix correction for models including realistic β-beat (dark/light purple), realistic linear coupling (dark/light orange), and upon application of best-knowledge alignment errors.

model. If $|f_{0030}|$ in the real LHC is significantly larger than expected from MB a_3 errors, compensation using only the existing MSS does not seem viable. Several alternatives can be considered: bypass of individual MSS to increase circuit influence on $3Q_y$, correction via orbit-bumps through octupoles, or correction with MCSSX. The latter case was tested in simulation (only single-beam compensation at flat-orbit was considered: dual-beam compensation with the common MCSSX correctors will require additional consideration).

Figure 4 shows simulation including measured nonlinear multipole errors in the arcs, effective models of nonlinear correctors used in operation, best-knowledge alignment errors applied to MB, MQ, MS, and Landau octupoles, with $|C^-| = 0.007$ and peak $\Delta\beta/\beta \approx 10\,\%$. Uncorrected f_{0030} was $\approx 5\times$ larger than models including only a_3 errors in MB. A **R**-matrix correction for $3Q_y$ using MSS and MCSSX was able to substantially reduce $|f_{0030}|$ while staying within powering limitations. While MSS settings were still significantly larger than the standard-correction (with corresponding risk to chromatic coupling), the majority of the correction is achieved via the MCSSX (which are located at significantly higher β_y at injection compared to MSS). The effect of turning off the MSS components of the correction are shown in Fig. 4 (black), and a significant reduction of $|f_{0030}|$ is still obtained, even without recalculating the correction. MCSSX correctors thus have sufficient strength at injection to facilitate compensation of even large f_{0030}. Operational complications however, may limit the use of MCSSX to dedicated studies, and dual-beam compensation requires further exploration. Use of MCSSX in such dedicated tests will be examined during the LHC's third run. The efficacy of corrections above were examined in PTC tracking simulations. Figure 5 shows on-momentum vertical phase-space before (top) and after (bottom) application of the MSS+MCSSX correction. Improvement to phase-space distortion is seen, with a clear reduction in the $3Q_y$ islands. Figure 6 shows surviving footprint after 20×10^3 turn tracking with corrected (blue) and uncorrected (dark red) models

ISBN: 978-3-95450-227-1 ISSN: 2673-5490 doi:10.18429/JACoW-IPAC2022-WEPOPT058

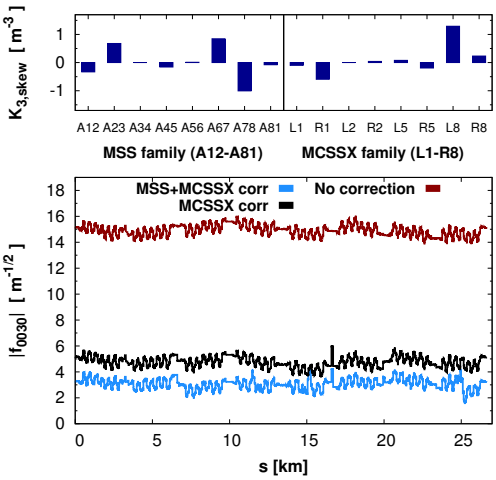

Figure 4: $|f_{0030}|$ before/after $\mathbf{R}$-matrix correction (bottom) with MSS and MCSSX (blue) and only MCSSX (black) for model scenario including magnetic, alignment, coupling, and β-beat errors. Corrector strengths are shown (top).

of Fig. 5. A notable reduction of the $3Q_y$ stop-band was achieved (tune diffusion via frequency map analysis [11–13] also showed clear improvement). f_{0030} was not perfectly compensated in Fig. 4 and losses are still observed at the $3Q_y$ resonance after correction, however it was expected from Fig. 3 that large β-beat and coupling present in the simulation would deteriorate correction quality. In the real LHC beam-based iteration may allow further improvement. Additionally higher-order multipoles present in the model also drive $3Q_y$ (via e.g. f_{1130},f_{0041}) which are not corrected by minimizing f_{0030}.

CONCLUSIONS

The LHC has no circuits designed for correction of $3Q_y$ at 450 GeV. Simulation studies were performed to attempt $3Q_y$ compensation (using what correctors do exist) via a response matrix determined from an ideal LHC model, acting only on f_{0030} at the BPMs. It was demonstrated in principle that such ideal-model based corrections, using only values at BPMs, did indeed enable $3Q_y$ correction. In practice however, using MSS correctors in the arcs it was found that only a moderate f_{0030} (on the scale induced by a_3 errors in main dipoles) could be compensated while remaining within powering limitations. Even with moderate f_{0030} further studies would be needed to assess the impact of chromatic-coupling induced by the strong MSS.

Analysis of models including measured LHC alignment errors indicated that such imperfections can give significant increases in the expected f_{0030}, compared to models including only measured multipole errors. It is aimed to check these predictions with beam during the upcoming LHC run. Correction of $3Q_y$ with the MSS is not viable in such scenarios, and alternative options for correction are being explored. In simulation, MCSSX in the experimental IRs were efficient at compensating the modelled $3Q_y$, however significant challenges exist to use in regular operation (particularly regarding simultaneous correction of both beams). None-the-less compensation via MCSSX can represent an interesting option for dedicated machine tests.

ACKNOWLEDGEMENTS

Many thanks go to R. Tomás and F.S. Carlier for their helpful discussions on this topic.

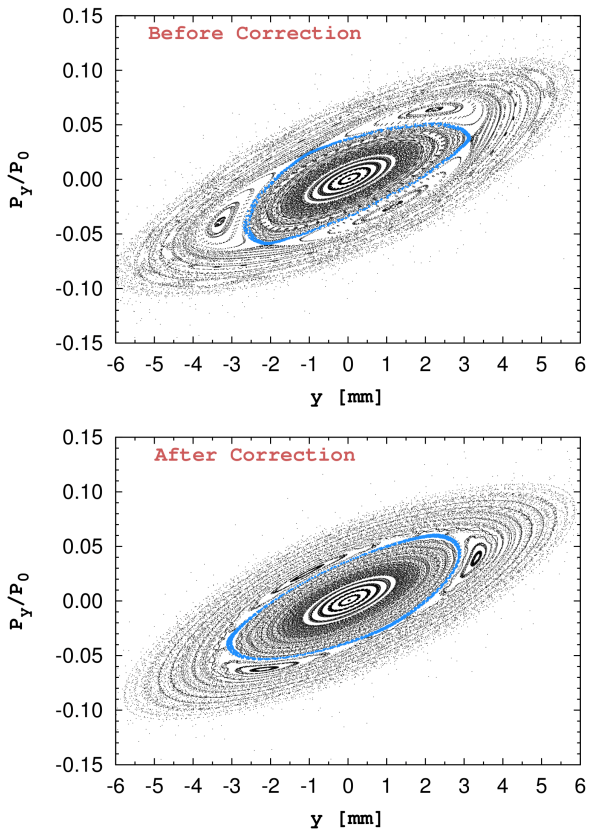

Figure 5: Tracking (at $\delta p/p = 0$) of vertical phase-space before (top) and after (bottom) correction of Fig. 4.

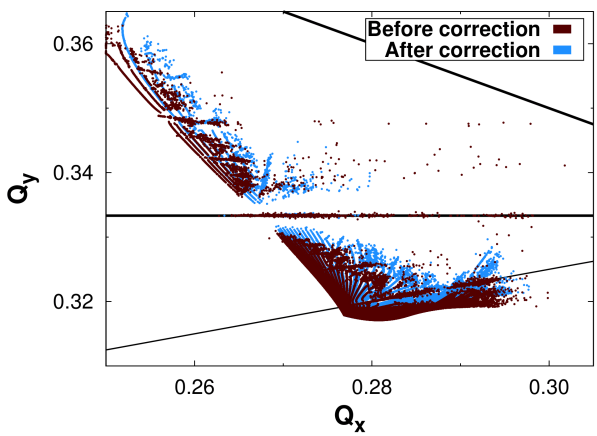

Figure 6: Comparision of Q-footprint after 20×10^3 Turn tracking simulation before (top) and after (bottom) application of $\mathbf{R}$-matrix correction of Fig. 4.

ISBN: 978-3-95450-227-1 ISSN: 2673-5490 doi:10.18429/JACoW-IPAC2022-WEPOPT058

REFERENCES

[1] E. H. Maclean, M. Giovannozzi, T. H. B. Persson, and R. Tomás García, "A Mechanism for Emittance Growth Based on Non-Linear Islands in LHC", in *Proc. IPAC'21*, Campinas, Brazil, May 2021, pp. 4082–4085. doi:10.18429/JACoW-IPAC2021-THPAB169

[2] S. Fartoukh and J. Koutchouk, "Chromatic copuling in the LHC and its correction," Tech. Rep., 2000, LHC Project Report 400. http://cdsweb.cern.ch/record/461473/files/lhc-project-report-400.pdf/

[3] S. Fartoukh, "Chromatic copuling in the LHC and its correction," Tech. Rep., 1998, LHC Project Report 278. http://cdsweb.cern.ch/record/383926/files/lhc-project-report-278.pdf/

[4] R. Wolf, "Field error naming conventions for LHC magnets," Tech. Rep., 2001, lHC-M-ES-0001 rev 3.0. https://lhc-div-mms.web.cern.ch/lhc-div-mms/tests/MAG/Fidel/

[5] T.H.B. Persson, Y. Levinsen, R. Tomás, and E.H. Maclean, "Chromatic Coupling Correction in the Large Hadron Collider," *Phys. Rev. ST. Accel. Beams*, vol. 16, p. 081003, 2013. doi:10.1103/PhysRevSTAB.16.081003

[6] E.H. Maclean, R. Tomás, F.S.. Carlier, M.S. Camillocci, J.W. Dilly *et al.*, "New approach to LHC optics commissioning for the nonlinear era," *Phys. Rev. Accel. Beams*, vol. 22, p. 061004, 2019. doi:10.1103/PhysRevAccelBeams.22.061004

[7] E.H. Maclean, R. Tomás, F.S. Carlier, M.S Camillocci, J. Coello de Portugal *et al.*, "Detailed review of the LHC optics commissioning for the nonlinear era," Tech. Rep., 2019, CERN-ACC-2019-0029. http://cds.cern.ch/record/2655741?ln/

[8] M. Benedikt, F. Schmidt, R. Tomás, and P. Urschutz, "Driving term experiments at CERN," *Phys. Rev. Accel. Beams.*, vol. 10, p. 034002, 2007. doi:10.1103/PhysRevSTAB.10.034002

[9] I.P.S. Martin, M. Apollonio, and R. Bartolini, "Online Suppression of the Sextupole Resonance Driving Terms in the Diamond Storage Ring", in *Proc. IPAC'16*, Busan, Korea, May 2016, pp. 3381–3384. doi:10.18429/JACoW-IPAC2016-THPMR001

[10] E. Waagaard, "Developing a Resonance Correction Scheme in the LHC," Tech. Rep., 2021, CERN-STUDENTS-Note-2021-017. https://cds.cern.ch/record/2778017/

[11] H. Dumas and J. Laskar, "Global dynamics and long-time stability in Hamiltonian systems via numerical frequency analysis," *Phys. Rev. Lett.*, vol. 70, no. 2975, 1993. doi:10.1103/PhysRevLett.70.2975

[12] J. Laskar, "Frequency Map Analysis and Particle Accelerators", in *Proc. PAC'03*, Portland, OR, USA, May 2003, paper WOAB001, pp. 378–382.

[13] Y. Papaphilippou, "Detecting chaos in particle accelerators through the frequency map analysis method," *Chaos*, vol. 24, p. 024412, 2014. doi:10.1063/1.4884495